SEE 2022

PROGRAMME & BOOK OF ABSTRACTS

8th INTERNATIONAL CONFERENCE ON SUSTAINABLE ENERGY AND ENVIRONMENT

THE ROAD TO NET-ZERO :
ENERGY TRANSITION CHALLENGES AND SOLUTIONS

7-9 November 2022,
THE KNOWLEDGE XCHANGE (KX), BANGKOK, THAILAND

Organisers

JGSEE

CEE
Center of Excellence on Energy Technology & Environment

KMUTT

Programme & Book of Abstracts

8th International Conference on
Sustainable Energy and Environment (SEE 2022)
"The Road to Net-Zero: Energy Transition Challenges and Solutions"

Published by The Joint Graduate School of Energy and Environment –
Center of Excellence on Energy Technology and Environment (JGSEE-CEE),
King Mongkut's University of Technology Thonburi (KMUTT)

Printed by Roy and Team Co., Ltd. Bangkok, Thailand

ISBN: 978-974-456-821-2

Printed in Thailand

Foreword

The Joint Graduate School of Energy and Environment (JGSEE-CEE), in collaboration with its consortium partners* and Kyoto University, is pleased to announce the organisation of the 8th International Conference on Sustainable Energy and Environment (hybrid) or "SEE 2022" on the theme "The Road to Net-Zero: Energy Transition Challenges and Solutions". The conference will be held during 7-9 November 2022 as a hybrid platform enabling participants to join virtually or in person at The Knowledge Xchange (KX) in Bangkok, Thailand.

The UN Climate Change Conference in Glasgow (COP26) last year reached a broad consensus on key actions to address climate change, including the science, solutions, political will to act, and clear indications of action. The conference produced new "building blocks" to advance the implementation of the Paris Agreement through actions that can get the world on a more sustainable, low-carbon pathway forward. Thus, more than 70 countries have set a target of reducing emissions to net-zero by 2050, covering about 76% of global emissions. Over 1,200 companies have put in place science-based targets in line with net-zero, and more than 1000 cities, over 1000 educational institutions, and over 400 financial institutions have joined the Race to Zero, pledging to take rigorous, immediate action to halve global emissions by 2030.

Since 2004, SEE, which is a series of biennial conferences, has been serving as a forum for presenting recent progress and advances in science, technology, and innovation that addresses energy, environment, and climate change issues, and exchange of ideas and networking. The SEE 2022 will continue to adhere to this theme. However, for this new edition of the SEE Conference, the emphasis will be on sustainable innovation and energy transition for accelerating solutions for climate actions in meeting net-zero emission ambitions by around mid-century and underpinning sustainable growth and development in the region and globally.

SEE 2022 will therefore serve as a forum for the exchange of information, knowledge and experiences in the field of smart city, future energy systems, bio-circular economy, environmental and climate technology management, and energy and climate science. Potential contributors from academia, research organizations, government agencies and international institutions, and private sector practitioners are invited to submit contributions in the areas of science, technology and policy, for on-site and virtual presentations at the conference.

Part of the highlights of the event includes the contribution during plenary sessions of internationally renowned keynote speakers in the field of energy and environment, and the inclusion among concurrent sessions of special sessions on (1) Waste Recycling and Waste Utilization: Covid 19 Aftermath, and (2) Roles of AFOLU in Net Zero Emission Development. This programme also contains abstracts of papers presented orally during the 3-day event.

I hope the readers find this programme & book of abstracts and the accompanying electronic copy of the proceedings, a useful source of information and reference.

Prof. Navadol Laosirpojana
Co-Chairperson of the Organizing Committee

Prof. Hideaki Ohgaki
Co-Chairperson of the Organizing Committee

Table of contents

Date: 9 November 2022 **Starting time: 13.30**

Topic D: Environmental and Climate Technologies and Management

Chairperson: Dr. Savitri Garivait

TIME	ROOM X11.4 (11th Floor, KX)	
13.30-13.40	**Introduction of the session by the chairperson**	
13.40-13.55	**Industrial electrification and its potential for deep decarbonization of manufacturing** *<u>Ali Hasanbeigi</u>, Jibran Zuberi, Lynn A. Kirshbaum, Blaine Collison*	**D1-03**
13.55-14.10	**The impacts of post-wildfire on streamflow and sediment dynamic in Mae Chaem river basin** *<u>Prangtip Triritthiwittaya</u>, Chaiwat Ekkawatpanit, Duangrudee Kositgittiwong, Amnat Chidthaisong*	**D1-11**
14.10-14.25	**Variations of urban heat island in a coastal city of Hat Yai, Thailand** *<u>Diem Kieu Nguyen</u>, Diem Kieu Phan, Can Trong Nguyen, Rungnapa Kaewthongrach, Sittiporn Channumsin, Mitchai Chongcheawchamnan*	**D1-14**
14.25-14.40	**Relationship of El Niño-Southern Oscillation and Indian Ocean Dipole on the winds and their effects on the hydrodynamic properties of the gulf of Thailand** *<u>Kittipong Phattananuruch</u>, Arachaporn Anutaliya, Anukul Buranapratheprat, Tanuspong Pokavanich*	**D1-15**

Topic E: Energy and Climate Policy

Chairperson: Dr. Suneerat Fukuda

TIME	ROOM X11.5 (11th Floor, KX)	
13.30-13.40	**Introduction of the session by the chairperson**	
13.40-13.55	**A possible carbon neutral energy system in 2050 Japan** *<u>Keiichi N. Ishihara</u>, Samuel M. G. Dumlao*	**E-16**
13.55-14.10	**Site suitability assessment for community-scale biomass power plant (CSBPP) development in the Eastern Economic Corridor (EEC) region using the MCDM-AHP method based on geospatial modeling platform** *<u>Athipthep Boonman</u>, Suneerat Fukuda, Agapol Junpen, Jompob Waewsak, Kanchit Ngamsanroaj, Pakorn Petchprayoon*	**E-04**
14.10-14.25	**Compensation rates of demand response program in Thailand** *<u>Anchisa Pinyo</u>, Athikom Bangviwat*	**E-06**
14.25-14.40	**The study of guideline for energy efficient buildings renovation: A case-study in Mechanical Building 4, King Mongkut's University of Technology Thonburi** *<u>Preecha Aregarot</u>, Kuskana Kubaha, Siriluk Chiarakorn*	**E-08**
14.40-14.45	**Applying blockchain technology to support electricity demand response in Thailand** *<u>Anchisa Pinyo</u>, Athikom Bangviwat*	**E-14**

****

DI-14

Variations of urban heat island in a coastal city of Hat Yai, Thailand

Diem Kieu Nguyen[1,2,3], Diem Kieu Phan[1,*], Can Trong Nguyen[2,3], Rungnapa Kaewthongrach[3,*], Sittiporn Channumsin[3], Mitchai Chongcheawchamnan[2]

[1]*College of Environment and Natural Resources, Can Tho University, Vietnam*
[2]*Faculty of Engineering, Prince of Songkla University, Thailand*
[3]*Space Technology Research Center, Geo-Informatics and Space Technology Development Agency, Thailand*

Abstract:
This study investigates patterns and characteristics of the surface urban heat island (SUHI) in Hat Yai City, a city located in Southern Thailand. In order to define urban and non-urban features from satellite images, an object-based classification was applied using Landsat 5 (TM) and Landsat 8 (OLI) for 2010 and 2020, respectively. Land surface temperature (LST) was extracted from the thermal infrared band of Landsat images as the main data sources for estimating SUHI variability over the period of 2010 and 2020. The spatial pattern and SUHI variation were then investigated using spatial analysis. The analysis of SUHI variation showed that the behaviour of LST depends on the land covers surrounding the city. In general, most LST in the urban areas were higher than surrounding areas in the study period. The response of SUHI to the increase in urban sites showed in both spatial and temporal variations. It indicates that SUHI intensity tends to slightly increase during 2010-2020 (about 0.41oC). Moreover, this study also pointed out that the densely built-up areas, and heavy industrial zones are the greatest contributors to SUHI of this city.

Keywords: Coastal Hatyai City; Land Surface Temperature; Songkhla Province; Surface Urban Heat Island

**Corresponding author. Tel: +66 844141625, E-mail address: rungnapa.kae@gistda.or.th, pkdiem@ctu.edu.vn*

Supporters

Ministry of Higher Education,
Science, Research and Innovation

Liberté • Égalité • Fraternité
RÉPUBLIQUE FRANÇAISE

AMBASSADE DE FRANCE
EN THAÏLANDE

CONTACT INFORMATION

SEE 2022 Secretariat
Partnership Relations and Outreach (PRO)
The Joint Graduate School of Energy and Environment,
King Mongkut's University of Technology Thonburi,
126 Prachauthit Road, Bangmod, Tungkru,
Bangkok 10140 Thailand

Tel: +66(0)2 470 8309-10 ext. 4130,
Fax: +66(02) 872 9805
Email: see.jgsee@gmail.com
Website: www.see-conf.com

ISBN : 978-974-456-821-2

8th International Conference on Sustainable Energy and Environment (SEE 2022):
The Road to Net-Zero: Energy Transition Challenges and Solutions
7-9 November 2022

Variations of urban heat island in a coastal city of Hat Yai, Thailand

Diem Kieu Nguyen[1,2,3], Diem Kieu Phan[1,*], Can Trong Nguyen[2,3], Rungnapa Kaewthongrach[3,*], Sittiporn Channumsin[3], Mitchai Chongcheawchamnan[2]

[1]*College of Environment and Natural Resources, Can Tho University, Vietnam*
[2]*Faculty of Engineering, Prince of Songkla University, Thailand*
[3]*Space Technology Research Center, Geo-Informatics and Space Technology Development Agency, Thailand*

Abstract:
This study investigates patterns and characteristics of the surface urban heat island (SUHI) in Hat Yai City, a city located in Southern Thailand. In order to define urban and non-urban features from satellite images, an object-based classification was applied using Landsat 5 (TM) and Landsat 8 (OLI) for 2010 and 2020, respectively. Land surface temperature (LST) was extracted from the thermal infrared band of Landsat images as the main data sources for estimating SUHI variability over the period of 2010 and 2020. The spatial pattern and SUHI variation were then investigated using spatial analysis. The analysis of SUHI variation showed that the behaviour of LST depends on the land covers surrounding the city. In general, most LST in the urban areas were higher than surrounding areas in the study period. The response of SUHI to the increase in urban sites showed in both spatial and temporal variations. It indicates that SUHI intensity tends to slightly increase during 2010-2020 (about 0.41°C). Moreover, this study also pointed out that the densely built-up areas, and heavy industrial zones are the greatest contributors to SUHI of this city.

Keywords: *Coastal Hatyai City; Land Surface Temperature; Songkhla Province; Surface Urban Heat Island.*

**Corresponding author. Tel: +66 844141625*
E-mail address: rungnapa.kae@gistda.or.th, pkdiem@ctu.edu.vn

1. Introduction

Climate change and socio-economic development are expected to amplify climate change risks. In Southeast Asia, occurrences of urban heat islands and extreme heat waves are a special concern for public health, well-being, and household energy consumption due to increased cooling demands (Nguyen et al., 2021). Urban heat island studies have revealed that Thailand's major cities are characterized by strong temperature differences between urban and rural areas (Nguyen et al., 2022). Therefore, understanding how surface urban heat island (SUHI) reacts in each typical city is paramount to propose adaptation measures and limiting adverse impacts on urban inhabitants. Using remote sensing techniques, various the land surface temperature and SUHI can be obtained by the Landsat, MODIS, and ASTER images (Liu and Zhang, 2011; Monteiro et al., 2021). However, in order to explore different aspects of urban heat island in the small region (city scale, district scale), Landsat is one of the reasonable satellite image that allows the user to analyze the surface temperature and its related features (land use/land cover) for a long period using spectral and thermal infrared bands (Popkin, 2018). Being the largest city in Southern Thailand and bordering Songkhla lake directly to the sea, this study takes Hat Yai as a coastal city to analyze the spatial temporal variations of surface urban heat island over 10 years (2010-2020) using the Landsat images.

2. Material and methods

2.1 Study area

Hat Yai is the largest city in Southern Thailand (Figure 1). Hat Yai has a population of 156,802 (2019) in the city and about 800,000 in the greater Hat Yai area (Department of Provincial Administration, Official Statistics Registration Systems, 2019). It is a popular destination for shopping and education, and serves as a hub for transportation and trading. Most of the destination place is built out or conserved as public open space. Predominant land uses include shopping malls and commercial streets, mixed-use neighborhoods, universities, public open spaces, and offices. The climate of the study area is influenced by tropical monsoons. The mean annual rainfall is approximately 2,216 mm, of which more than 50% falls during the northeast monsoon season from October to January (Tabucanon et al., 2021).

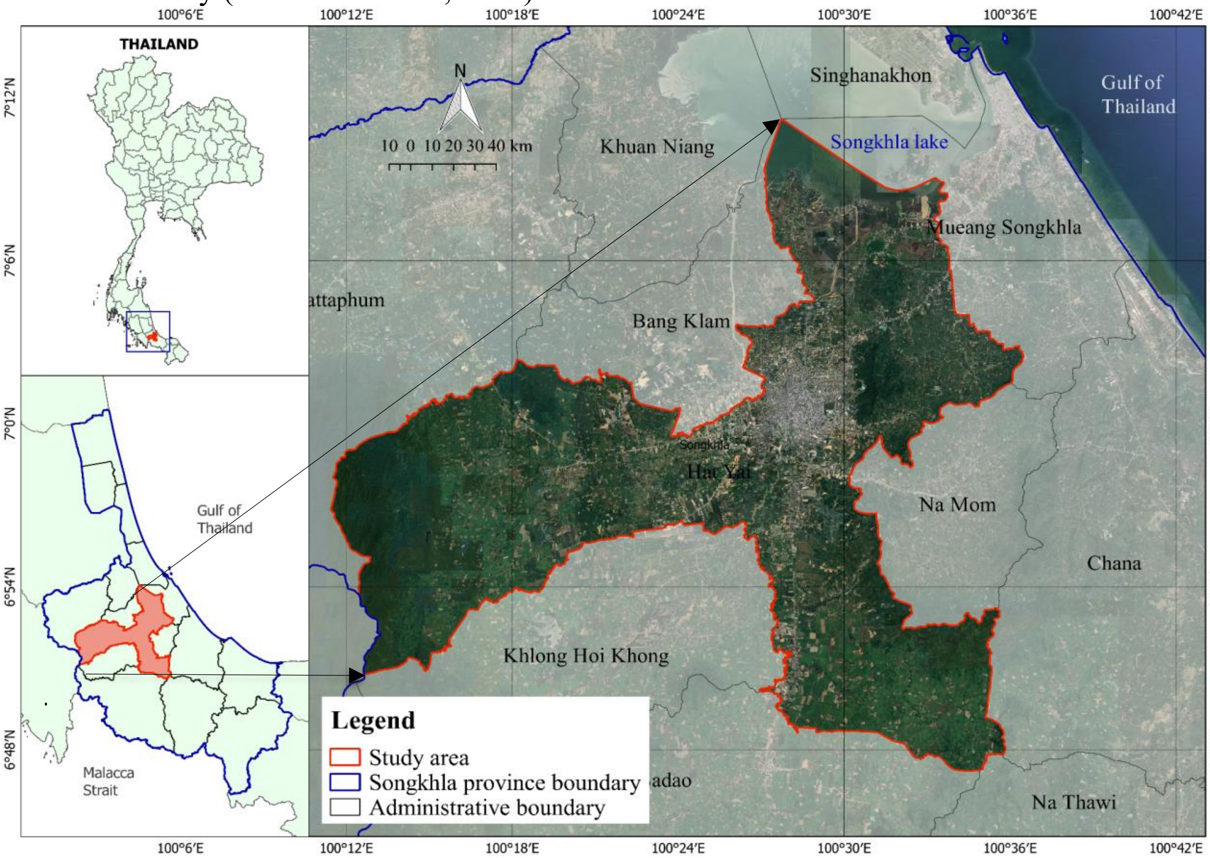

Fig. 1 Location of study area

2.2 Data collection

This study used Landsat images with a spatial resolution of 30 m. Landsat 5 TM acquired on 07/05/2010 and Landsat 8 OLI acquired on 19/06/2020 were downloaded via United States Geological Survey (USGS) website (https://earthexplorer.usgs.gov/). Landsat spectral bands were used for classifying the land use and identifying the urban and non-urban areas, while Landsat thermal infrared bands were used for LST extraction.

2.3 Methods

2.3.1 Image pre-processing

The collected Landsat images were preprocessed by the following steps: (1) Region of interest using Hat Yai boundary (shapefile); (2) Radiometric correction using Radiometric Calibration tool (Schowengerdt, 2007); (3) Atmospheric correction was conducted by using Fast Line-of-sight Atmospheric Analysis of Hypercubes-FLAASH method (Kaufman et al., 1988).

2.3.2 Land cover classification

Multiresolution segmentation was applied by setting up three main components such as scale parameter (4), shape (0.1), and compactness (0.5). This approach divides remote sensing images into sub-regions called contours by merging the neighbour pixels that have consistency on spectrals and spatial distribution (Kok et al., 1999). This algorithm is not only based on the spectral reflectance of the objects, but also on the color, size, position, shape and contextual characteristics between each object (Chen et al., 2019).

An object-based classification was used to classify the urban and non-urban areas based on spectral band indices as Normalized Difference Vegetation Index (NDVI, Eq.1), Normalized Difference Built-up Index (NDBI, Eq.2) (Table 1).

Table 1 Spectral indices used in land cover features classification

Index	Range	Sources	Equation (Eq.)
$NDVI = \frac{pNIR-pRED}{pNIR+pRED}$	(-1 to 1)	Tucker, (1979)	(Eq.1)
$NDBI = \frac{pSWIR1 - pNIR}{pSWIR1 + pNIR}$	(-1 to 1)	Zha et al., (2003)	(Eq.2)

2.2.3 Accuracy assessment

The reliability of classification was assessed by the Kappa coefficient (K) and overall accuracy (T) based on the confusion matrix using ground truth points. This study was carried out in the period 2010-2020, the ground truth points are selected randomly based on Google Earth image data using Historical function. Number truth points were decided depending on the proportion of each land use type, whereas a minimum of each class is 50 points (Finegold et al., 2016). In this study, a total of 152 samples were collected as the validation dataset of Landsat images.

2.2.4 Derivation of land surface temperature (LST)

In order to calculate the land surface temperature, the thermal infrared – TIR bands were used to identify the value of spectral radiance (L_λ), brightness temperature (T_B), and land surface emissivity (LSE).

(i) Spectral radiance (L_λ) was obtained as Eq. (3):

$$L_\lambda = M_L \times Q_{CAL} + A_L \quad \text{(Eq.3)} \qquad \text{(USGS, 2016)}$$

Where: L_λ is a spectral radiance ($W \times m^{-2} \times sr^{-1} \times \mu m^{-1}$); M_L: radiance multiplicative scaling factor obtained from the metadata by *RADIANCE_MULT_BAND_x* value; A_L: radiance additive scaling factor obtained from the metadata by *RADIANCE_ADD_BAND_x* value; QCAL: the image pixel value.

(ii) Brightness temperature (T_B) was proposed by Xu and Chen, (2004) presented in Eq. (4):

$$T_B = K_2/\ln (K_1/L_\lambda + 1) \quad \text{(Eq.4)}$$

Where:

T_B is the brightness temperature (°K); K_1 and K_2 are thermal conversion constants from the metadata; L_λ is the spectral radiance that was obtained by Eq. (3).

(iii) Land surface emissivity (LSE) was identified using the vegetation fraction (Golub et al., 1999). LSE_{TM} was calculated by Eq. (5), while LSE_{OLI} was followed as Eq. (6) according to the separate empirical formula for each sensor (Jiang et al., 2004).

$$LSE_{TM} = 0.004 \times Pv + 0.986 \qquad \text{(Eq.5)}$$

$$LSE_{OLI} = 0.00149 \times P_v + 0.986481 \qquad \text{(Eq.6)}$$

Pv is the vegetation fraction that was estimated based on the NDVI index (Xu & Shen, 2013) as Eq. (7), whereas NDVI is the pixel value of vegetation on the image, $NDVI_{min}$ and $NDVI_{max}$ are minimum and maximum value of the NDVI image, respectively.

$$P_v = [(NDVI - NDVI_{min})/(NDVI_{max} - NDVI_{min})]^2 \quad \text{(Eq.7)}$$

(iv) Land surface temperature (LST) was computed by adjusting the brightness temperature using LSE as follows:

$$LST = [T_B /(1+ \lambda \times T_B /C_2) \times \ln(LSE)] – 273.15 \quad \text{(Eq.8)}$$

Where: λ is the wavelength of emitted radiance (μm); C_2 is a coefficient calculated as formula hc/s (1.4388×10^{-2} mK), h is planck's constant (6.626×10^{-34} Js), s is Boltzmann constant (1.38×10^{-23} JK^{-1}), c is the velocity of light (2.998×10^8 ms^{-1})

2.2.2 Computing urban heat island (UHI)

According to the land surface temperature distribution maps, the surface urban heat island was then defined based on the characteristics of the LST. In particular, the urban heat island was identified as a difference of LST between the urban areas in comparison with non-urban areas, in which the LST in the urban areas are warmer than the surrounding non-urban environment (Eq.9).

$$LST > T_{mean} + 0.5 \times S_d \qquad \text{(Eq.9)}$$

Where T_{mean} is the average temperature in the study area; S_d is the standard deviation.

3. Results and discussion

3.1 Land cover maps

The result of land cover classification was obtained by an object-based approach, which fastly showed a change in built-up, water, green space and others (mainly vegetation), especially in the built-up area. The land cover in Hat Yai was mapped for the year of 2010, 2020 (Figure 2). In general, built-up expansion was found due to the tendency of decreasing the green space over study period (Figure 2-yellow rectangles). However, there are some typical points that are maintained as green space during 10 years observed. In particular, the rubber farm (Figure 2-green rectangles), Hat Yai municipal park, and moist evergreen forest on the mountain covering the large green area which could contribute to reduce heat and other negative effects at daytime.

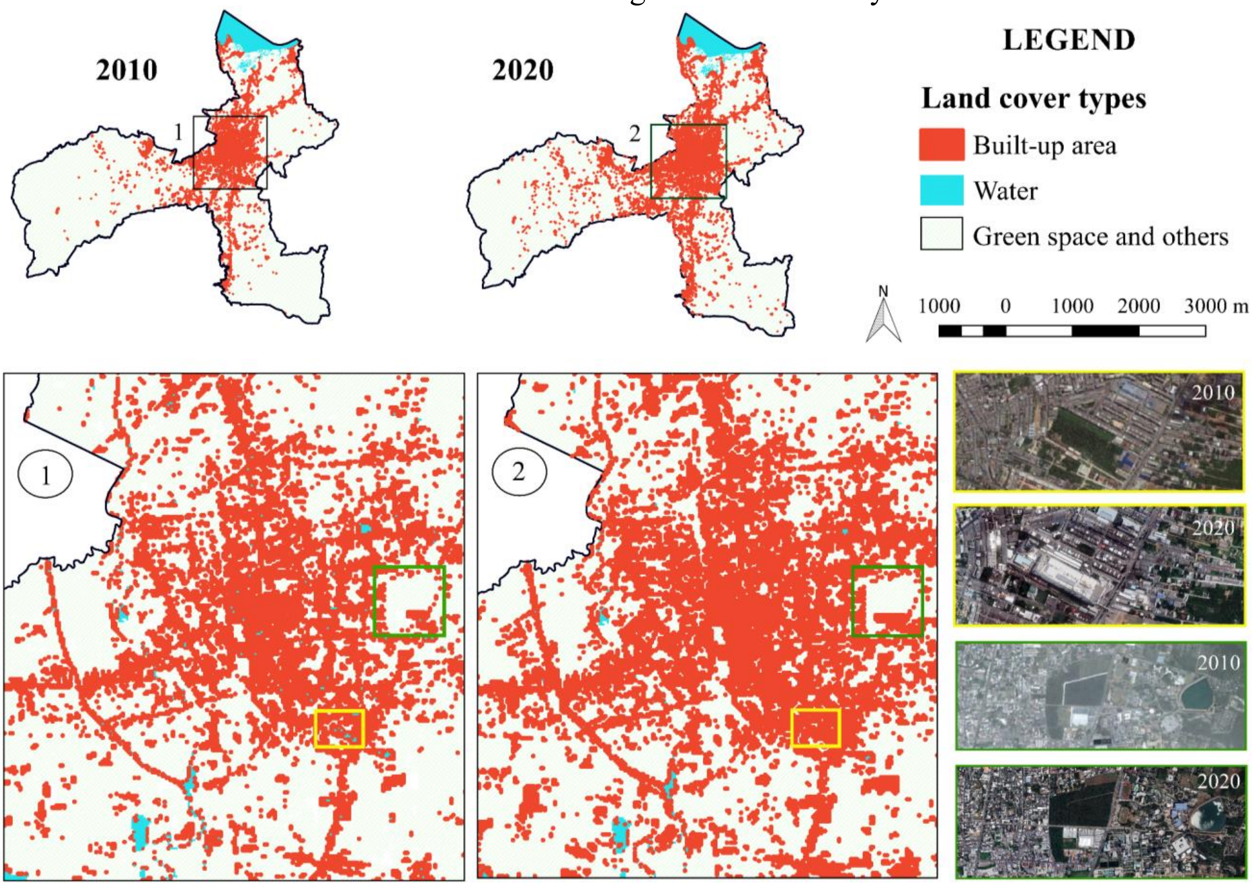

Fig. 2 Classified land cover maps in the period 2010-2020

The accuracy for each classified image was evaluated using quantitative metrics, including the overall accuracy and kappa coefficient. A total 152 ground truth points were used for accuracy assessment of land cover classified. The overall accuracy ranges from 80% to 90%, kappa coefficient values were greater than 0.79. In 2010, the accuracy of land cover map was relatively low (84.1%) in comparison with the year of 2020 (88.8%) due to cloud cover in some specific areas leading to difference in reflectance values for each object. Total areas of each land cover type reflected a clearly increasing trend in terms of built-up areas from 2.62% in 2010 to 3.22% in 2020 (426.33 ha of expansion) for the entire study area. In contrast, the green space areas significantly decreased, a total area of 468.71 ha of vegetated area was converted into other land uses from 2010 to 2020. Green space mainly composed of agricultural lands in surrounding areas was changed into construction land due to urbanization as well as the pressure from other land use applications.

3.2 Variations of land surface temperature

Figure 3 showed the vivid changes in land surface temperature magnitude in Hat Yai during the study period. In 2010, the average temperature was found at 25.25°C while it slightly increased to 25.81°C after 10 years. Generally, LST was rising mostly in the inner city (Figure 3-black oval) and other expansion areas, the highest temperature pointed out at 38.98°C. However, LST of the area bordering Songkhla lake and Mueang Songkhla district in the East was suddenly changed in the study period. This area is located in the agricultural region, which means that the land cover can vary with the seasons. Therefore, LST value variations depend on the vegetation proportion at the time of acquiring the Landsat images.

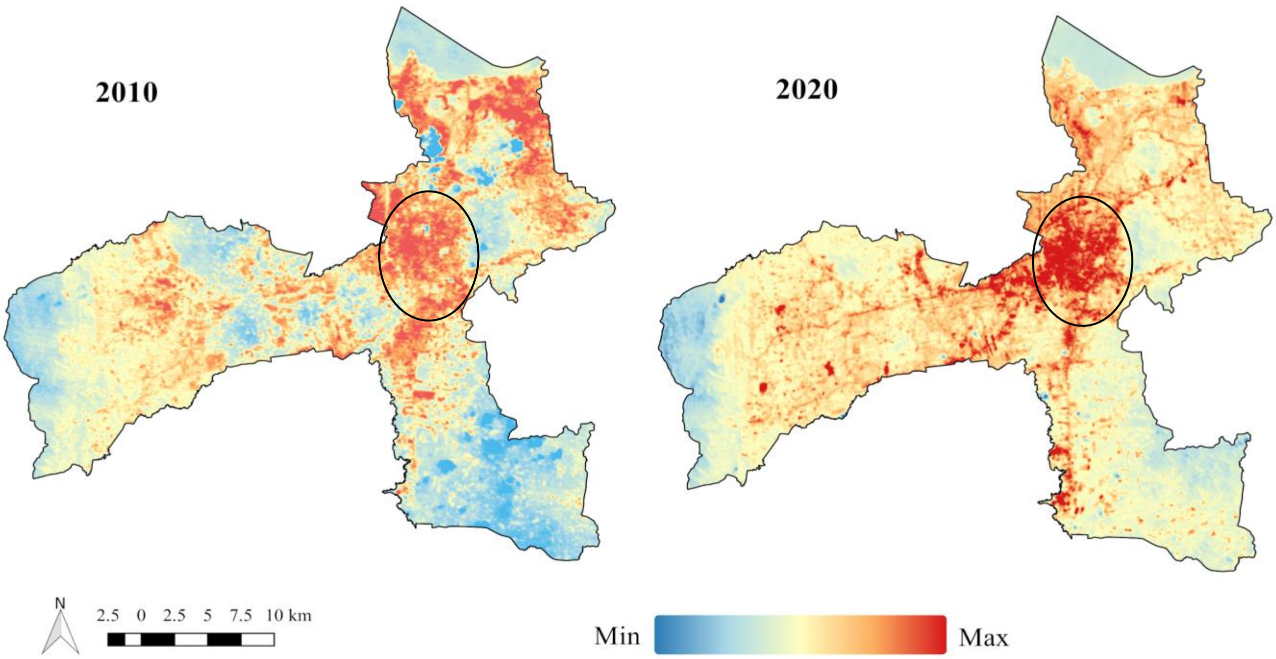

Fig. 3 Land surface temperature spatial pattern in the study area for period of 2010-2020

3.3 Surface urban heat island distribution

Hat Yai nevertheless remains an interesting study site due to the specific characteristics of the local climate, despite its relatively low urban proportion compared to the total areas. According to the LST retrieval results, the spatial distribution of SUHI was illustrated in Figure 4. The SUHI intensity obviously increased during the 10 years period. The expansion of the SUHI corresponds to the urban spatial growth patterns. According to the sprawl of urban built-up lands, new hot spots of heat island appeared in the newly built areas surrounding the city center. The SUHI intensity in the study area increased 0.41°C in the period of 2010-2020 according to the mean values (Table 2).

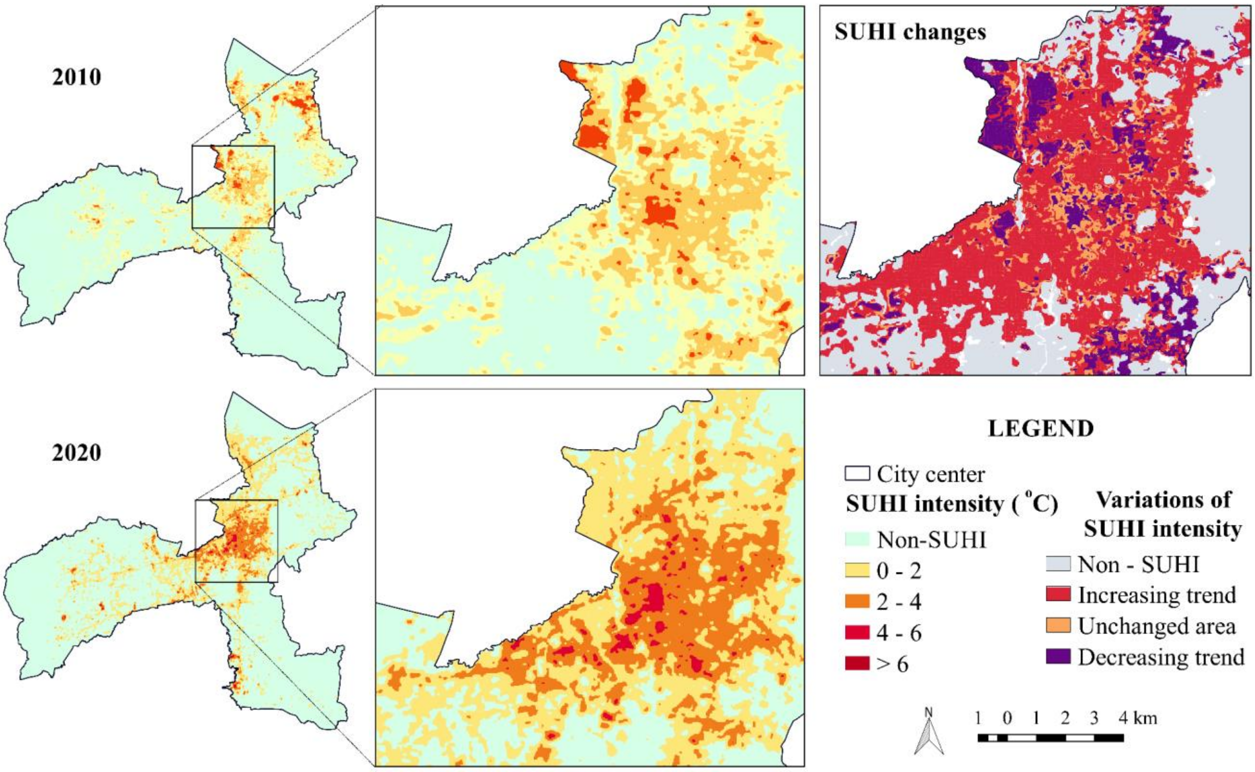

Fig. 4 Spatial pattern of SUHI intensity in Hat Yai from 2010 to 2020

Surface urban heat island areas accounted for 547.56 ha rising from the beginning to the end of study period. The areas have increased in SUHI intensity mainly located in the central city with high population density and built up area (Figure 4). Besides, the ratio of SUHI areas was also calculated with more than 25% (Table 2). Research indicated that the overall surface urban heat island magnitude was gradually increasing in both spatial and temporal dimensions.

Table 2 The statistical data present the SUHI intensity in Hat Yai city

Year	The average of SUHI intensity (°C)	Total areas effects (ha)	The ratio of SUHI areas (%)
2010	2.41	20,011.95	25.46%
2020	2.82	20,559.51	26.16%

The increasingly directional changes of land cover in the impervious areas play an essential role in affecting the heat island intensity in the city. An urban cross-sectional heat island analysis of 3 km has been applied in typical hot spot areas for understanding the heat island variation over the past 10 years. The first cross-section (location 1) represents the densely built-up areas such as commercial, communication and other services, while the second cross-section (location 2) represents the industrial zone in the surrounding area. The black and green curves show the complex behaviour of SUHI after ten years changes (Figure 5). However, the SUHI intensity generally begins to increase between 1.5°C and 3.7°C in the new construction areas toward the end of the period (black and green triangles).

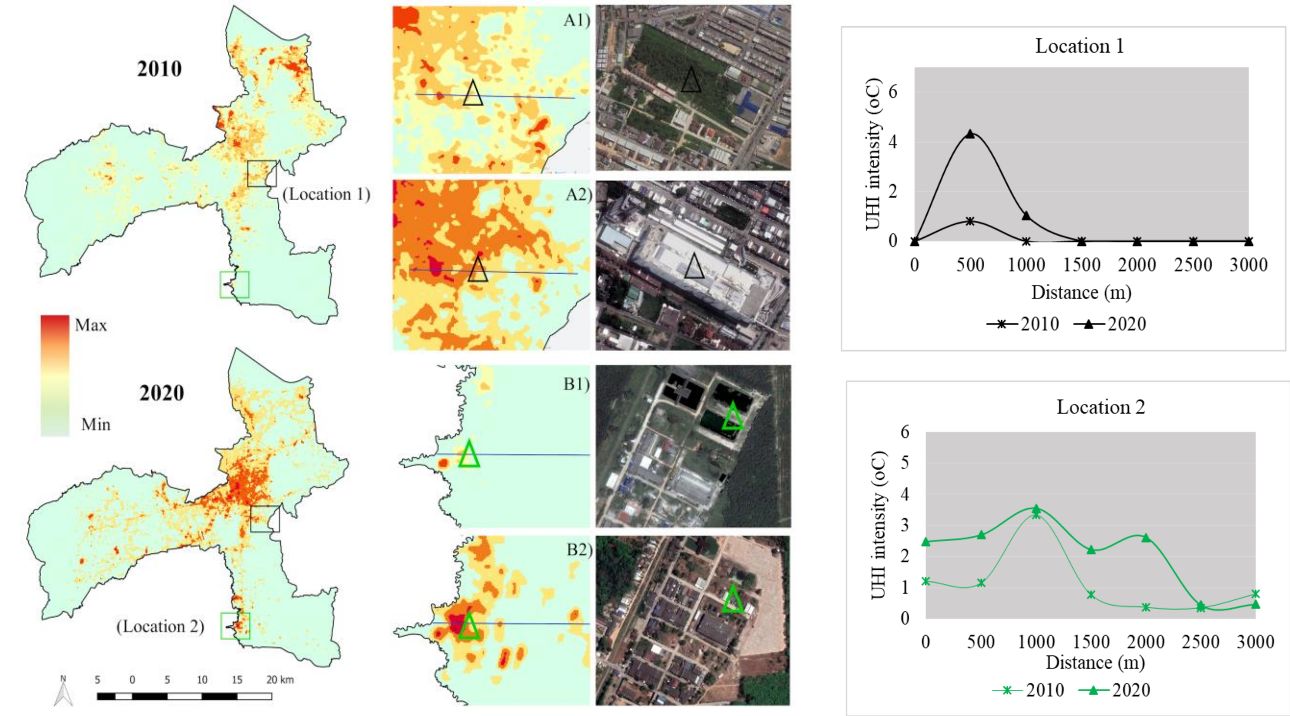

Fig. 5 Urban heat island intensity fluctuation in the typical hot spot areas (A1, A2: Zoom-in at location 1 in 2010, 2020 respectively; B1, B2: Zoom-in at location 2 in 2010, 2020 respectively)

According to the Green city action plan for Hat Yai Municipality, Hat Yai has considerable small and medium size industries located within the municipal boundary (Asian Development Bank, 2015). Development of the industrial zones, commercial,... has been actively contributed to the social-economic aspects in this city. However, as a primary result of this paper, it's important to consider thermal effects and urban heat island variations for long-term sustainable development.

4. Conclusion

In this research, Landsat imagery has been used to study the spatial and temporal variation of SUHI occurrence in Hat Yai city, Thailand. The following conclusions were made: (1) the land cover maps pointed out a change in built-up, water, green space over study period, especially the built-up area with more than 400 ha of expansion; (2) Urban areas have increased in the study area and contributed to the variations of the spatial and temporal LST and affected the UHI intensity primarily through urban sprawl, human activities,… (3) UHI intensity has slightly increased in the period 2010-2020 in both spatial and temporal dimensions. Result implied that the spatial arrangement impacts of urban areas and features of green space on urban thermal environments should be further investigated. Afterwards, the research outcomes allow policymakers and planners to better understand the spatial distribution of SUHI in this city for developing the SUHI mitigation strategies for building a green city, promoting more sustainable and resilient urban development.

Acknowledgement

This research was supported by the Space Technology Research Center, Geo-Informatics and Space Technology Development Agency (GISTDA), Chonburi 20230, Thailand. Additionally, the Department of Public Works and Town & Country Planning Songkhla Office is also acknowledged for supporting all the urban data in Hat Yai city.

References

Asian Development Bank. 2015. Green City Action Plan for Songkhla and Hat Yai Municipalities. Available at: https://www.adb.org/sites/default/files/related/41572/imt-gt-green-city-action-plan-songkhla-hat-yai-municipalities-march-2015.pdf

Chen, Y., Chen, Q., & Jing, C. 2019. Multi-resolution segmentation parameters optimization and evaluation for VHR remote sensing image based on mean NSQI and discrepancy measure. Journal of Spatial Science, 66(2), 253-278. DOI: 10.1080/14498596.2019.1615011

Department of Provincial Administration, Official Statistics Registration Systems. 2019. The population of Hat Yai city. Available at: http://citypopulation.de/en/thailand/southern/songkhla/9098__hat_yai/

Finegold, Y., Ortmann, A., Lindquist, E., d'Annunzio, R., Sandker, M. 2016. Map Accuracy Assessment and Area Estimation: A Practical Guide; Food and Agriculture Organization of the United Nations: Rome, Italy

Golub, T. R., Slonim, D. K., Tamayo, P., Huard, C., Gaasenbeek, M., Mesirov, J. P., Coller, H., Loh, M. L., Downing, J. R., Caligiuri, M. A., Bloomfield, C. D., Lander, E. S. 1999. Molecular classification of cancer: class discovery and class prediction by gene expression monitoring. Science 286.

Jiang, H., Deng, Y., Chen, H., Tao, L., Sha, Q., Chen, J., Tsai, C., and Zhang, S. 2004. Joint analysis of two microarray gene expression data sets to select lung adenocarcinoma marker genes. BMC Bioinformatics 5.

Kaufman, Y. J., & Sendra, C. 1988. Automatic atmospheric correction. Int. J. Remote Sensing, 9, 1357-1381. https://doi.org/10.1080/01431168808954942

Kok, R. D., Schneider, T., & Ammer, U. 1999. Object based classification and applications in the Alpine forest environment. International Archives of Photogrammetry and Remote Sensing, 32(7), 4-3

Liu, L., and Zhang, Y. 2011. Urban heat island analysis using the Landsat TM data and ASTER Data: A case study in Hong Kong. Remote Sensing, 3(7), 1535–1552. https://doi.org/10.3390/rs3071535

Monteiro, F. F., Gonçalves, W. A., Andrade, L. D. M. B., Villavicencio, L. M. M., & dos Santos Silva, C. M. 2021. Assessment of Urban Heat Islands in Brazil based on MODIS remote sensing data. Urban Climate, 35, 100726.

Nguyen, C. T., Chidthaisong, A., Limsakul, A., Varnakovida, P., Ekkawatpanit, C., Diem, P. K., & Diep, N. T. H. 2022. How do disparate urbanization and climate change imprint on urban thermal variations? A comparison between two dynamic cities in Southeast Asia. *Sustainable Cities and Society*, *82*, 103882. https://doi.org/10.1016/J.SCS.2022.103882

Nguyen, C. T., Diep, N. T. H., & Diem, P. K. 2021. Factors affecting urban electricity consumption: a case study in the Bangkok Metropolitan Area using an integrated approach of earth observation data and data analysis. *Environmental Science and Pollution Research*, *28*, 12056–12066. https://doi.org/10.1007/s11356-020-09157-6

Popkin, G. 2018. The US government considers charging for popular Earth-observing data. Nature, 556 (7702), 417–418. doi:10.1038/d41586-018-04874-y

Schowengerdt, R. A. 2007. Correction and calibration. Remote Sensing (Third edition), 285–354, XVI-XXIII. doi:10.1016/B978-012369407-2/50010-3

Tabucanon, A. S., Kurisu, K., & Hanaki, K. 2021. Assessment and mitigation of tangible flood damages driven by climate change in a tropical city: Hat Yai Municipality, southern Thailand. *Science of The Total Environment*, 789, 147983.

Tucker, C. J. 1979. Red and photographic infrared linear combinations for monitoring vegetation. https://doi.org/10.1016/0034-4257(79)90013-0

USGS. 2016. Landsat 8 (L8) Data Users Handbook (LSDS-1574 version 2.0). USGS Landsat User Services. U.S. Geological Survey.

Wang, Z., Gang, C., Li, X., Chen, Y., & Li, J. 2015. Application of a normalized difference impervious index (NDII) to extract urban impervious surface features based on Landsat TM images. International Journal of Remote Sensing, 36(4), 1055-1069.

https://doi.org/10.1080/01431161.2015.1007250

Xu, H. 2010. Analysis of impervious surface and its impact on Urban heat environment using the normalized difference impervious surface index (NDISI). Photogramm. Eng. Remote Sensing, 76, 557–565. https://doi.org/10.14358/PERS.76.5.557

Xu, Y., and Shen, Y. 2013. Reconstruction of the land surface temperature time series using harmonic analysis. Computers & Geosciences 61, 126-132

Zha, Y., Gao, Y., & Ni, S. 2003. Use of normalized difference built-up index in automatically mapping urban areas from TM imagery. International Journal of Remote Sensing, 24, 583–594. https://doi.org/10.1080/01431160304987